REPORT DOCUMENTATION PAGE

Form Approved OMB NO. 0704-0188

1. REPORT DATE (DD-MM-YYYY)	2. REPORT TYPE	3. DATES COVERED (From - To)
01-05-2012	Conference Proceeding	-

4. TITLE AND SUBTITLE
Characterization of electrical properties of polymers for conductive nano-composites

5a. CONTRACT NUMBER
W911NF-08-1-0350

5b. GRANT NUMBER

5c. PROGRAM ELEMENT NUMBER
611102

6. AUTHORS
Oliver K. Johnson, Daniel Seegmiller, David T. Fullwood, Andrew Dattelbaum, Nathan A., Mara, George Kaschner, Thomas Mason

5d. PROJECT NUMBER

5e. TASK NUMBER

5f. WORK UNIT NUMBER

7. PERFORMING ORGANIZATION NAMES AND ADDRESSES
Brigham Young University
ORCA
Brigham Young University
Provo, UT 84602 -1231

8. PERFORMING ORGANIZATION REPORT NUMBER

9. SPONSORING/MONITORING AGENCY NAME(S) AND ADDRESS(ES)
U.S. Army Research Office
P.O. Box 12211
Research Triangle Park, NC 27709-2211

10. SPONSOR/MONITOR'S ACRONYM(S)
ARO

11. SPONSOR/MONITOR'S REPORT NUMBER(S)
54633-MS.29

12. DISTRIBUTION AVAILIBILITY STATEMENT
Approved for public release; distribution is unlimited.

13. SUPPLEMENTARY NOTES
The views, opinions and/or findings contained in this report are those of the author(s) and should not contrued as an official Department of the Army position, policy or decision, unless so designated by other documentation.

14. ABSTRACT
Properties of various conductive nano-composites are dominated by quantum-level effects across small barriers created by the matrix material. The properties of the matrix clearly have a vital influence on the resultant behavior of the material. However, the quantification of the relevant matrix properties at the quantum level is difficult to measure using current techniques. This paper reports on recent work to simplify the process of characterizing the electrical properties of

15. SUBJECT TERMS
Nano composites, piezo-resistivity, quantum tunneling

16. SECURITY CLASSIFICATION OF:			17. LIMITATION OF ABSTRACT	15. NUMBER OF PAGES	19a. NAME OF RESPONSIBLE PERSON
a. REPORT	b. ABSTRACT	c. THIS PAGE			David Fullwood
UU	UU	UU	UU		19b. TELEPHONE NUMBER: 801-422-6316

Report Title

Characterization of electrical properties of polymers for conductive nano-composites

ABSTRACT

Properties of various conductive nano-composites are dominated by quantum-level effects across small barriers created by the matrix material. The properties of the matrix clearly have a vital influence on the resultant behavior of the material. However, the quantification of the relevant matrix properties at the quantum level is difficult to measure using current techniques. This paper reports on recent work to simplify the process of characterizing the electrical properties of various polymers at this length scale using a nano-indenter with a conductive tip.
A brief overview of the physical theory behind the technique is presented, along with preliminary experimental results. Though the technique shows significant sensitivity to data analysis procedures, the measured values agree reasonably well with those available in the literature. The methodology provides key insights into the behavior of conductive nanocomposites of various types.

Conference Name: SAMPE 2011

Conference Date: May 22, 2011

CHARACTERIZATION OF ELECTRICAL PROPERTIES OF POLYMERS FOR CONDUCTIVE NANO-COMPOSITES

Oliver K. Johnson[1], Daniel Seegmiller[1], David T. Fullwood[1], Andrew Dattelbaum[2], Nathan A. Mara[2], George Kaschner[3], Thomas Mason[3]

[1]Brigham Young University
Provo, UT 84602
[2]Center for Integrated Nanotechnologies
Los Alamos, NM 87544
[3]Los Alamos National Laboratory
Los Alamos, NM 87544

ABSTRACT

Properties of various conductive nano-composites are dominated by quantum-level effects across small barriers created by the matrix material. The properties of the matrix clearly have a vital influence on the resultant behavior of the material. However, the quantification of the relevant matrix properties at the quantum level is difficult to measure using current techniques. This paper reports on recent work to simplify the process of characterizing the electrical properties of various polymers at this length scale using a nano-indenter with a conductive tip.

A brief overview of the physical theory behind the technique is presented, along with preliminary experimental results. Though the technique shows significant sensitivity to data analysis procedures, the measured values agree reasonably well with those available in the literature. The methodology provides key insights into the behavior of conductive nano-composites of various types.

1. INTRODUCTION

Charge transport in conductive polymer composites (CPCs) whose filler concentration is close to the percolation threshold (and where the excitation voltage is less than that required for dielectric breakdown) is dependent upon quantum mechanical phenomena such as electron tunneling [1-4]. Previous experiments to quantify a critical parameter for this mode of charge transport, the tunneling barrier height, have been performed for vacuum, aqueous barriers and biological molecules [5-8]. These experiments have used STM and AFM techniques which lend themselves readily to these systems. However, to our knowledge no robust method for measurement of barrier heights in bulk solids currently exists. Given the increasing importance of nano-scale electrical devices, which depend on quantum mechanical charge transport, a need exists for such a characterization tool. We have developed a conductive nanoindentation technique capable of measuring the tunneling barrier height for a wide range of materials and systems. We share preliminary results on several polymeric materials, however, there is no theoretical limitation to solids—this technique should be applicable to materials of all phases.

2. THEORY

In a conductor-insulator-conductor junction the tunneling barrier height, λ, is the energy difference between the conduction band of the insulator—the lowest unoccupied molecular orbital (LUMO)—and the conduction band of the conductor (i.e. the work function of the conductor, ϕ) (Fig. 1). If the conductors are dissimilar the system will have one barrier on either side of the insulator, λ_1 and λ_2, respectively. Incident charge carriers (we restrict our discussion to electrons, but the theory is applicable to holes as well) with energy greater than λ are able to pass freely into the conduction band of the insulator and therefore travel *over* the barrier. In the classical regime, electrons with energy less than λ are reflected; however, if the barrier width is sufficiently small, the solutions of the one-dimensional time-independent Schrödinger equation give a finite probability for transmission of the electrons *through* the barrier. The electrical conductance of tunneling junctions is inversely proportional to the transmission coefficient from the Schrödinger equation and can be expressed as [5]:

$$G_t = G_0 \exp\left(-1.025\sqrt{\bar{\lambda}}s\right) \tag{1}$$

Where G_t is the tunneling conductance in micro-Siemens (μS), s is the barrier width in Å, $\bar{\lambda}$ is the apparent barrier height in eV, and G_0 is the conductance for a zero barrier width (i.e. contact conductance). When a voltage potential is applied to the system the energy required to raise an electron from one of the conductors to the vacuum level is increased. If the applied voltage is not too great this has the effect of changing the shape of the barrier from a rectangular barrier (a basic assumption of the classic 1D tunneling model), to a trapezoidal barrier (Fig. 2). As a result, there is an *apparent barrier height* given by (adapted from [9]):

$$\bar{\lambda} = \frac{\lambda_1 + \lambda_2 - \Delta eV}{2} \tag{2}$$

Where ΔeV is the net potential difference across the junction (in Fig. 2, $\Delta eV = eV_s - eV_0$). By measuring the conductance across a tunneling junction (G_t) as a function of the barrier width (s), we are able to deduce the apparent barrier height as:

$$\bar{\lambda} = \left[\frac{d(\ln(G_t))/ds}{-1.025}\right]^2 \tag{3}$$

In other words, the apparent barrier height is proportional to the square of the slope of the $\ln(G_t)$ vs. s plot. Using a conductive nanoindenter tip and substrate with a thin-film of insulating material, we have characterized the G_t vs. s behavior of various polymers, and hence, their apparent tunneling barrier heights.

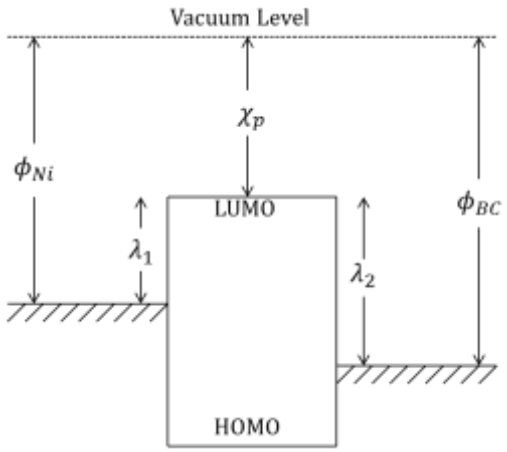

Figure 1: Electronic band diagram for a Ni-polymer-B-doped Diamond tunneling junction. χ_p is the electron affinity of the insulating material; ϕ_{Ni} and ϕ_{BC} are the work functions of the Ni and B-Doped Diamond respectively; and λ_1, λ_2 are the real potential barrier heights for incident electrons from either side of the barrier.

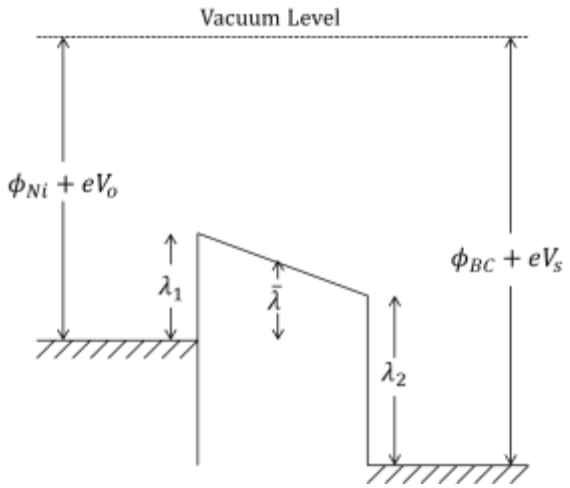

Figure 2: Electronic band diagram for the same system as shown in Fig. 1, with voltage potentials applied according to the system setup of the present experiment. e is the elementary charge of an electron; V_0 is the output voltage (see Fig. 4); V_s is the supply voltage (see Fig. 4); and $\bar{\lambda}$ is the apparent barrier height.

3. METHODS

3.1 Sample Preparation

Thin-films of poly(dimethylsiloxane) (PDMS)—Sylgard® 184, polyethylene glycol (PEG), polyvinylpyrrolidone (PVP), and a thermoplastic polyurethane (TPU)—Estane®, were applied using spin and dip coating methods to commercially pure nickel plates of dimensions 40mm x 20mm x 1mm. Prior to applying the thin-films, the plates were mechanically polished, cleaned with methanol, dried under a spray of nitrogen, and then exposed to ultraviolet radiation in order to burn off any hydrophobic organic matter that could adversely affect adhesion of the films. After spin coating, the samples were cured at 100°C for over 12 hours.

The thin-films were characterized using ellipsometry and all were found to be between 6-15nm in thickness (Table 1).

Table 1: Film thicknesses as characterized by ellipsometry.

Polymer	Thickness (nm)
PDMS	8
PEG	7-11
PVP	8-15
TPU	9

3.2 Conductive Nanoindentation

A single tunneling junction was simulated by a nickel plate—upon which a polymer thin-film was deposited—and a boron-doped diamond nanoindenter tip of cube corner geometry (Fig. 3). A sample holder for the MTS Nanoindenter XP system was fabricated out of polytetrafluoroethylene (PTFE) to which the nickel plate was adhered so as to insulate the nickel plate from the test fixture. The top of the nanoindenter tip was covered with a thin layer of poly(4,4'-oxydiphenylene-pyromellitimide) tape and the tip holder nut was fabricated from PTFE in order to insulate it from the test fixture as well. In this way we electrically isolated our region of interest. A Stanford Research Systems SR830 lock-in amplifier was used to excite the circuit with a 1 kHz AC signal of 1 V_{rms} magnitude. Use of the lock-in amplifier allowed us to isolate our signal by only picking up voltage signals with matching frequency and phase to that of supplied signal. The lock-in amplifier has an input impedance of $R_{in} = 10$ MΩ; in order to determine the tunneling resistance, R_t, (and hence G_t) the potential drop across R_{in} was measured simultaneously and synchronously with the displacement of the nanoindenter tip as it penetrated the thin-film (Figs. 4,5).

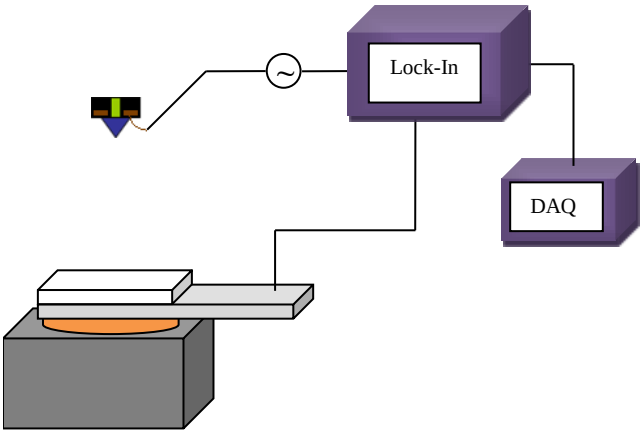

Figure 3: Schematic diagram of the conductive nanoindentation tunneling experiment. The various components are as follows: Lime – poly(4,4'-oxydiphenylene-pyromellitimide) Tape; Brown – Cu Washer; Black – PTFE Tip Nut; Purple – B-doped Diamond Tip; White Box – Polymer Thin-film; Light Grey Box – Nickel Plate; Orange – PTFE Puck; Dark Grey Box – Indenter Puck Holder.

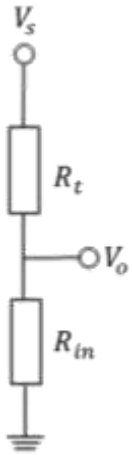

Figure 4: Schematic circuit diagram for the conductive nanoindentation tunneling experiment. V_s is the supply voltage; V_0 is the measured output voltage (i.e. the potential drop across the gap between the tip and the substrate); R_t is the resistance of the tunneling junction; R_{in} is the input impedance of the lock-in amplifier (10MΩ).

Theoretically one could derive R_t directly from the measured output voltage as in (see Fig. 4):

$$R_t = \frac{(V_s - V_o)}{V_o} R_{in} \tag{4}$$

However, capacitive effects caused by the shielding in the BNC cables rendered this kind of analysis impossible. In order to accurately convert V_o to R_t, calibration measurements were

performed by replacing the indenter tip/thin-film/nickel plate component of the circuit (i.e. R_t) with known resistors from 1Ω to 2×10^9Ω and recording the corresponding output voltage. Using this calibration data (Fig. 5), R_t was able to be accurately recovered.

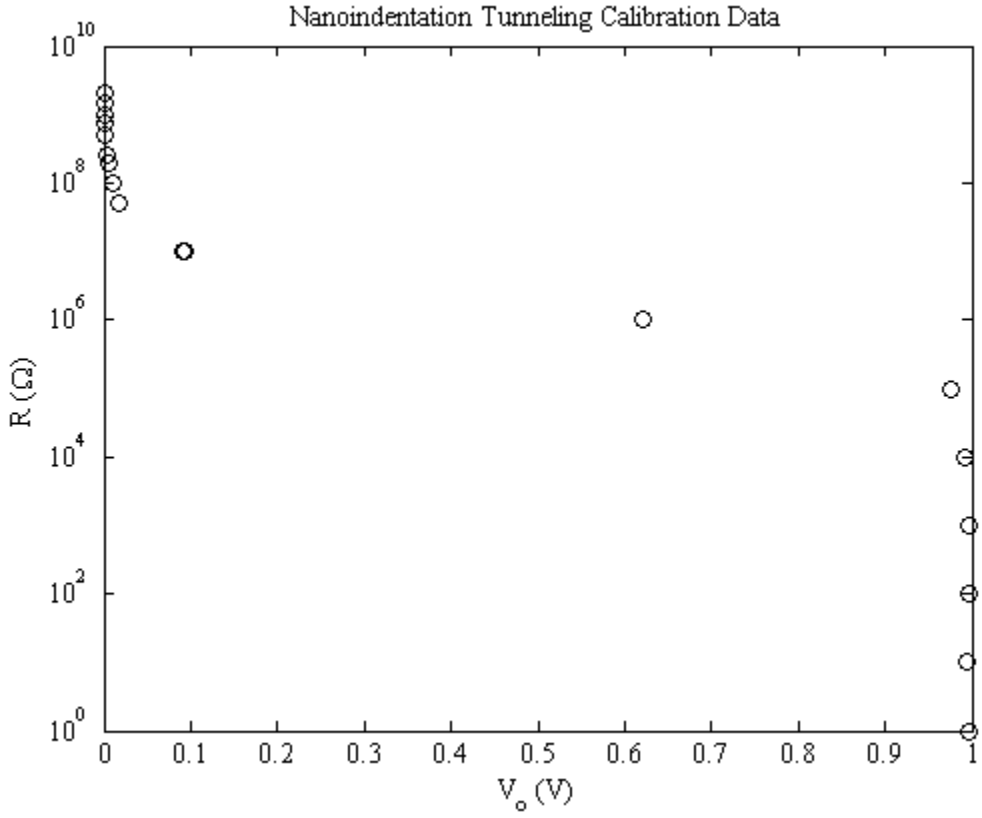

Figure 5: Calibration data for the conductive nanoindentation tunneling experiment.

4. RESULTS

Figure 6 shows the tunneling current (I_t) and tunneling voltage (V_t) results (i.e. the potential drop across s) for a representative trial of each of the polymers tested. A test was also performed on a bare Ni substrate for comparison with literature values. As the tip displacement (z) increases (decrease in s), and the tip begins to penetrate the surface of the thin-film, I_t increases exponentially, while V_t decreases exponentially. This exponential change occurred over a distance of ~1nm for all materials except the PEG and TPU, which varied over a slightly larger distance, agreeing well with other tunneling experiments and the 1D tunneling model [5]. Because of the compliance of the polymeric thin-films and the fact that the conventional indentation method was used (as opposed to the Continuous Stiffness Method), the location of the film surface was difficult to identify, which precluded direct measurement of s. However, as can be seen from Eq. 3, derivation of $\bar{\lambda}$ requires only the measurement of ds, and since $dz = -ds$, this does not present any obstacle to the measurement of $\bar{\lambda}$.

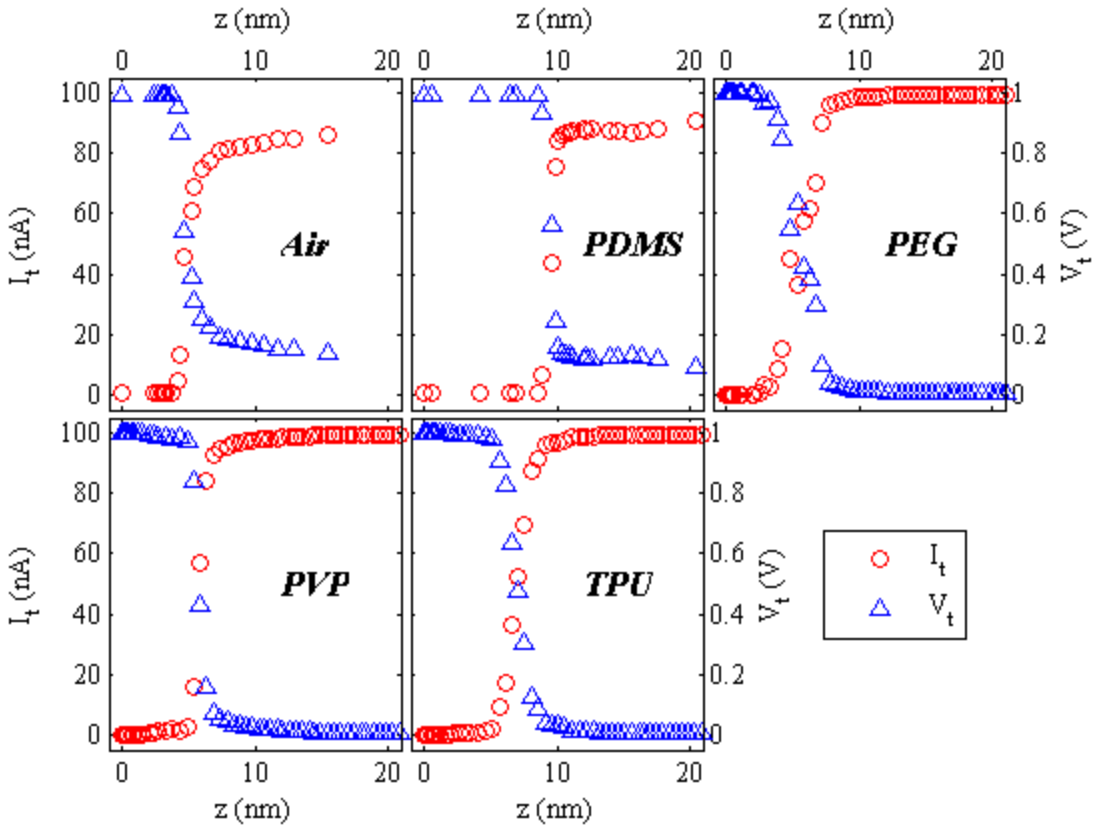

Figure 6: Tunneling current (I_t) and tunneling voltage (V_t) results as a function of tip displacement (z).

As stated previously $\bar{\lambda}$ was calculated from the slope of the $\ln(G_t)$ vs. s plot and Eq. 3 (see Fig. 7).

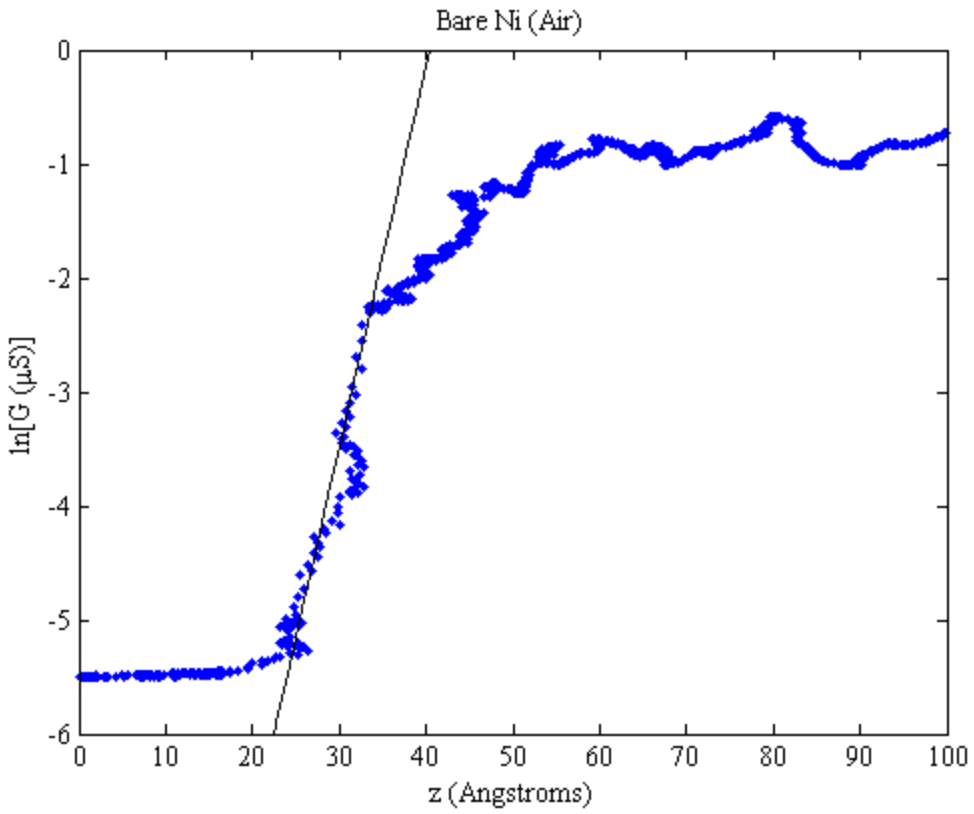

Figure 7: Example plot of $\ln(G_t)$ vs. z in air (i.e. with no film), illustrating how the tunneling barrier height is deduced from the slope of the linear portion of the plot.

The measured barrier heights for all of the tests are shown in Fig. 8. The barrier height of air, as determined by our measurements, was ~0.3eV, which is somewhat lower than typical values reported by other authors (in the range of 0.6-1.5eV [10]). As such, the barrier heights that we measured for the other materials might also be slightly low. We note that other authors have reported anomalous low barrier heights in electrochemical STM experiments (as compared to $\bar{\lambda}$ in vacuum) [5]. As discussed in [5], there are several postulated explanations for abnormally low barrier heights, including the possibility of Ohmic leakage currents. Additionally, we found that the obtained barrier height values were highly sensitive to the portion of the data that was considered and it was often difficult to identify the appropriate region of the $\ln(G_t)$ vs. s plot from which to take the slope. However, the measurements showed reasonable repeatability, and the data clearly shows the exponential increase in tunneling conductivity as predicted by the 1D tunneling model. We suggest the following improvements for future work: (1) use of the continuous stiffness method to accurately identify the location of tip-surface contact, (2) development of a more systematic method for identifying the correct region of the $\ln(G_t)$ vs. s from which to take the slope.

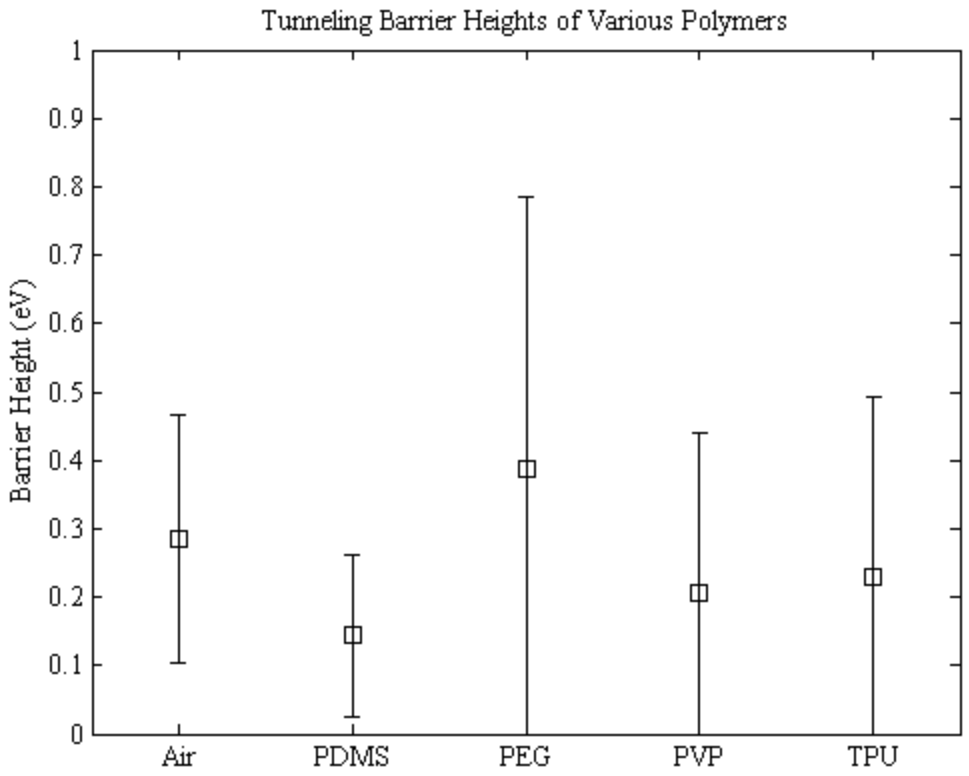

Figure 8: Experimental results of tunneling barrier heights for each of the materials tested. The weighted average for all trials is given along with error bars showing ± one weighted standard deviation. Weights were assigned based on the R^2 value of the linear fit, the range of z over which the data was taken, and the quality of the experimental data.

5. CONCLUSIONS

We have developed a new conductive nanoindentation technique capable of characterizing the quantum mechanical barrier height of solid materials. Preliminary results are encouraging, but show significant sensitivity to data analysis procedures. These results will lead to significant insight into the properties of conductive nano-composites.

6. ACKNOWLEDGEMENTS

The authors are grateful to the Joint DoD/DOE Munitions Technology Development Program for support of this work.

This work was performed, in part, at the Center for Integrated Nanotechnologies, a U.S. Department of Energy, Office of Basic Energy Sciences user facility at Los Alamos National Laboratory (Contract DE-AC52-06NA25396) and Sandia National Laboratories (Contract DE-AC04-94AL85000).

The authors would also like to thank John Yeager for performing the ellipsometric characterization of the thin-films, and Phillip Rae for his assistance in designing and building the circuitry for the test fixture.

7. REFERENCES

1. Hu, N et al. “Tunneling effect in a polymer/carbon nanotube nanocomposite strain sensor.” *Acta Materialia* 56.13 (2008): 2929-2936.
2. Kyrylyuk, A.V., and P. van Der Schoot. “Continuum percolation of carbon nanotubes in polymeric and colloidal media.” *Proceedings of the National Academy of Sciences* 105.24 (2008): 8221.
3. Radhakrishnan, S., S. Chakne, and Pn Shelke. “High piezoresistivity in conducting polymer composites.” *Materials letters (General ed.)* 18.5-6 (1994): 358–362.
4. Rakowski, Wieslaw, and Marcin Kot. “Thermal Stress Model for Polymer Sensors.” *Journal of Thermal Stresses* 28.1 (2004): 17-28.
5. Woo, D-H. et al. “Current–distance–voltage characteristics of electron tunneling through an electrochemical STM junction.” *Surface Science* 601.6 (2007): 1554-1559.
6. Lee, Nam-suk et al. “Study on tunneling current through barrier height using scanning tunneling microscopy.” *2006 IEEE Nanotechnology Materials and Devices Conference* (2006): 570-571.
7. Engelkes, Vincent B, and C Daniel Frisbie. “Simultaneous nanoindentation and electron tunneling through alkanethiol self-assembled monolayers.” *The journal of physical chemistry. B* 110.20 (2006): 10011-20.
8. Yamada, Yoichi et al. “Local Tunneling Barrier Height Measurement on Au(111).” *Japanese Journal of Applied Physics* 42.Part 1, No. 7B (2003): 4898-4900.
9. "John G. Simmons Formula in a Case of Small, Intermediate and High Voltage (Field Emission Mode)." *1.2.2 John G. Simmons Formula in a Case of Small, Intermediate and High Voltage (Field Emission Mode) - NT-MDT.* NT-MDT, Moscow, Russia. 1/29/2011 <http://www.ntmdt.com/spm-basics/view/different-modes>.
10. Ahn, J., and M. Pyo. “Comparison of STM Barrier Heights on HOPG in Air and Water.” *Bulletin of the Korean Chemical Society* 21.6 (2000): 644-646.